RAPID COMMUNICATIONS

PHYSICAL REVIEW B VOLUME 46, NUMBER 23 15 DECEMBER 1992-I

Theory of the quantum confinement effect on excitons in quantum dots of indirect-gap materials

Toshihide Takagahara and Kyozaburo Takeda
NTT Basic Research Laboratories, Musashino-shi, Tokyo 180, Japan
(Received 13 April 1992)

The quantum confinement effect on excitons in quantum dots of indirect-gap materials is investigated and a mechanism that induces an indirect-to-direct conversion of the character of the optical transition is clarified. The exciton transition energy and the exciton binding energy are calculated and found to be in good agreement with experimental results on Si and Ge nanostructures. The large exciton binding energy in Si and Ge quantum dots suggests that the photoluminescence from these nanostructures is of excitonic origin even at room temperature. The estimated radiative lifetime of excitons is strongly size dependent and varies from nanosecond to millisecond corresponding to the diameter from ~ 10 to ~ 30 Å. These theoretical results suggest strongly the importance of the quantum confinement effect in the luminescence processes of porous Si.

Recently, a great deal of research effort was focused on the low-dimensional structures of indirect-gap materials such as Si,[1-7] Ge,[8,9] and AgBr.[10,11] Especially, in the last few years, the visible photoluminescence from porous Si has attracted much attention from the fundamental physics viewpoint and from the interest of the potential application to optical devices. The mechanism of the photoluminescence is the main issue of the current research and is still controversial at the present stage. The blueshift of the photoluminescence was observed when the Si column size was reduced by increasing the etching time duration in HF solution.[3] This observation suggests the presence of the quantum confinement effect in Si nanostructures. On the other hand, the importance of the localized levels at the surface of nanostructures in the photoluminescence was pointed out by several authors.[5] The visible photoluminescence was observed also from Ge quantum dots.[9] Because the mechanism of photoluminescence from nanostructures of indirect-gap materials is controversial and not well understood, it is important to clarify theoretically the intrinsic optical properties of excitons in these quantum-confined structures. The comparison of the theoretical results with experimental data will shed a new light on the mechanism of photoluminescence. In this paper, we investigate the quantum confinement effect on excitons in nanostructures of indirect-gap materials and calculate the exciton transition energy, exciton binding energy, and exciton oscillator strength or radiative lifetime.

In the bulk crystal of indirect-gap materials, the electron-hole recombination is possible only through phonon emission or absorption because the wave-vector difference between the conduction-band bottom and the valence-band top must be compensated. One of the most effective means to convert an indirect optical transition into a direct one is to form a superlattice structure[12-15] by which the size of the Brillouin zone is reduced and the conduction-band bottom is folded onto the Γ point, resulting in a direct-gap material. On the other hand, in nanostructures such as an isolated quantum dot, the periodicity due to a superstructure is absent and the above picture of zone folding is not applicable straightforwardly. In these structures, the electronic states become completely discrete as in atoms and molecules and the optical matrix element between a pair of discrete states must be evaluated to identify whether that transition is optically allowed or not. This is the most legitimate picture. However, in a relatively large nanostructure, we can employ approximately the picture of zone folding. If the envelope functions of carriers confined in a nanostructure have a sizable Fourier component at the wave vector corresponding to the indirect-gap transition, that Fourier component plays the same role as phonons in the bulk material and the direct optical transition becomes allowed. This mechanism of luminescence is similar to that of a bound exciton trapped by nitrogen impurities in GaP.[16]

The electronic structures of linear chain and planar polysilanes were calculated by the first-principles method and interesting optical properties were predicted.[17] Here, in order to see more conveniently the dependence of excitonic optical properties on the nanostructure size, we employ the effective-mass approximation.[18] Concerning the morphology of porous Si, recent studies suggest that the structure is a network of interconnected nanocrystallites rather than a series of parallel columns.[5] Here, in order to simplify the analysis but to retain the essential physics, we consider an isolated nanocrystallite or more specifically a spherical quantum dot and calculate the excitonic states using the Luttinger Hamiltonian[19] for the valence band. The mass anisotropy at the conduction-band bottom is also included. The valley degeneracy of the conduction band is taken into account in the calculation of the excitonic radiative lifetime. The conduction-band minimum is located at $k_0=2\pi/a(0,0,0.85)$ and another five equivalent points in the case of Si and at $k_0=\pi/a(1,1,1)$ and another three equivalent points for Ge, where a is the lattice constant.[20] The energy disper-

sion around this point is given as

$$K_c=\frac{\hbar^2}{2m_{\parallel}}(k_{\parallel}-k_0)^2+\frac{\hbar^2}{2m_{\perp}}k_{\perp}^2 , \quad (1)$$

where $k_{\parallel}$ ($k_{\perp}$) is the wave-vector component in the direction parallel (perpendicular) to the vector k_0 and $m_{\parallel}$ ($m_{\perp}$) is the corresponding component of mass tensor. The kinetic-energy part of the valence-band Hamiltonian for the $j=\frac{3}{2}$ multiplet in the spherical approximation[21] is given as

$$K_v=-\frac{\gamma_1}{2m_0}\left[p^2-\frac{\mu}{9}(P^{(2)}J^{(2)})\right] , \quad (2)$$

where $\mu=(4\gamma_2+6\gamma_3)/5\gamma_1$ and γ_1, γ_2, and γ_3 are the Luttinger parameters, m_0 is the free electron mass, $P^{(2)}$ and $J^{(2)}$ are second-rank tensors composed of the orbital momentum operator and the angular momentum operator ($j=\frac{3}{2}$), respectively, and $(P^{(2)}J^{(2)})$ is a scalar product between the two second-rank tensors. Then the relevant Hamiltonian for the excitonic state becomes

$$\begin{aligned}H_X&=H_e^{(0)}+H_h^{(0)}-\frac{e^2}{\epsilon|r_e-r_h|}\\&=-\frac{\hbar^2}{2m_{\parallel}}\nabla_{e\parallel}^2-\frac{\hbar^2}{2m_{\perp}}\nabla_{e\perp}^2+V_e(r_e)\\&\quad+\frac{\gamma_1}{2m_0}\left[p_h^2-\frac{\mu}{9}(P_h^{(2)}J^{(2)})\right]+V_h(r_h)-\frac{e^2}{\epsilon|r_e-r_h|} ,\end{aligned} \quad (3)$$

where the subscript e (h) is attached to the quantities associated with the electron (hole), $H_e^{(0)}$ corresponds to the first three terms in the last line, $H_h^{(0)}$ to the next two terms, the confinement potentials V_e and V_h are assumed to be infinitely high outside the quantum dot, and ϵ is the dielectric constant of the quantum dot material. The lowest excitonic state can be constructed from a product of the lowest subband functions of the electron and the hole and a function describing the electron-hole relative motion. Since the Hamiltonian (3) has an axial symmetry around the k_0 direction, which will be referred to as the z direction, the z component of the total angular momentum of the excitonic state is a good quantum number. The lowest subband state of the electron has an even parity with respect to the center of the quantum dot and is given as

$$f_e(r_e)=Y_{00}(\Omega_e)\varphi_0(r_e)+Y_{20}(\Omega_e)\varphi_2(r_e)+\cdots , \quad (4)$$

where Y_{lm} is a spherical harmonics and φ_0 and φ_2 are the radial part envelope functions. The lowest subband state of the hole is an eigenstate of $H_h^{(0)}$ and is given as

$$\begin{aligned}f_h(r_h;S_{3/2})&=g_0(r_h)|l=0,j=\tfrac{3}{2},F=\tfrac{3}{2},F_z\rangle\\&\quad+g_2(r_h)|l=2,j=\tfrac{3}{2},F=\tfrac{3}{2},F_z\rangle ,\end{aligned} \quad (5)$$

where l denotes the orbital angular momentum and F is a combined angular momentum of l and j. The radial part envelope functions g_0 and g_2 as well as φ_0 and φ_2 in (4) satisfy the boundary condition that they vanish at the quantum dot surface and are expanded in terms of $j_l(k_j^l r/R)$ where R is the radius of the spherical quantum dot and k_j^l is the jth zero of the spherical Bessel function $j_l(z)$. In order to find out the lowest excitonic state, we employ a variational envelope function[22] as

$$\Phi(r_e,r_h)=N_{\Phi}e^{-\alpha|r_e-r_h|}f_e(r_e)f_h(r_h;S_{3/2}) , \quad (6)$$

where N_{Φ} is the normalization constant and the variational parameter α optimizes the electron-hole relative motion. The exciton binding energy is defined by $B_X=E_e+E_h-E_X$, where E_X is the exciton energy and E_e and E_h are the subband energies corresponding to (4) and (5), respectively.

The calculated exciton energy and the exciton binding energy are shown as a function of the quantum dot radius in Figs. 1 and 2, respectively, for Si and Ge. From the comparison of Fig. 1 with the peak energy of photoluminescence spectra of Ref. 3, it seems likely that Si nanostructures with diameter about 50–65 Å are formed in the samples. Furthermore, the exciton binding energy corresponding to this range of quantum dot size is estimated to be about 75–95 meV. These values are in good agreement with the experimentally measured activation energy from the temperature dependence of the photoluminescence intensity.[23] A strong room-temperature photoluminescence was observed from Ge nanocrystals embedded in SiO_2 glassy matrices.[9] The luminescence peak energy of 2.18 eV corresponds to the quantum dot diameter of about 42 Å, as can be estimated from Fig. 1. This value is consistent with the average size estimated by means of Raman spectroscopy and high-resolution electron microscopy.

The enhancement factor of the exciton binding energy

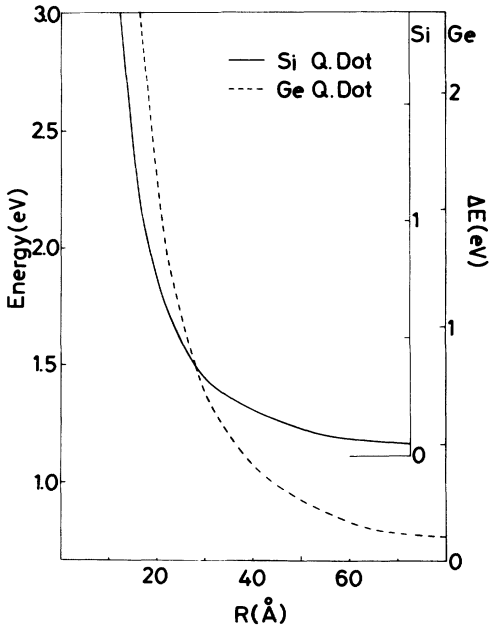

FIG. 1. The exciton energy in quantum dots is plotted as a function of the dot radius for Si (solid line) and Ge (dashed line). The right ordinate indicates the confinement energy ΔE measured from the indirect band-gap energy of the bulk material.

relative to the bulk value (Ry^*) is shown on the right ordinates of Fig. 2. The enhancement factor of Ge is larger than that of Si for the same size of quantum dot, as expected from the lighter carrier masses in Ge.[24] Since the exciton Bohr radius in the bulk material is generally larger for the case of lighter carrier masses, the quantum confinement effect appears more pronounced in Ge than in Si.

Now we discuss the oscillator strength or the radiative lifetime of excitons. In view of the large exciton binding energy, the photoluminescence is likely to be of excitonic origin rather than arising from the recombination of free-electron–hole pairs. Experimentally, the photoluminescence decay dynamics show a nonexponential behavior with typical time constants ranging from nanosecond (ns) to millisecond (ms).[5] This behavior suggests strongly the presence of inhomogeneous size distribution of Si nanostructures and also the presence of nonradiative relaxation channels of excitons. Thus it is very important to investigate theoretically the exciton lifetime due to the intrinsic radiative recombination and its dependence on the luminescence wavelength or the nanocrystallite size, since we can identify the dominant luminescence mechanism from the comparison between the theory and experiments.

The momentum matrix element of the excitonic transition is calculated as

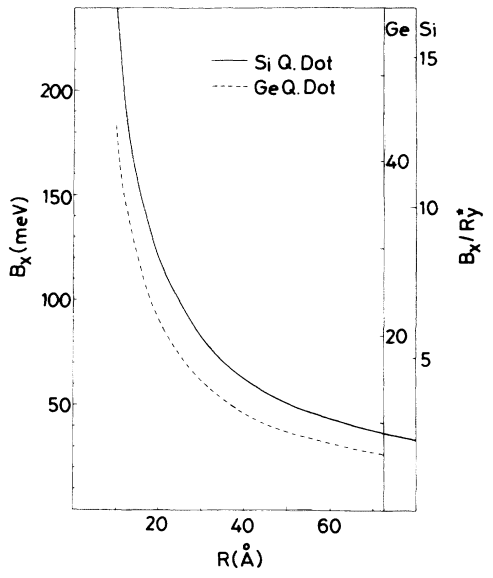

FIG. 2. The exciton binding energy in quantum dots is plotted as a function of the dot radius for Si (solid line) and Ge (dashed line). The right ordinate represents the same quantity normalized by the exciton binding energy (Ry^*) in the bulk material. This ratio indicates the strength of the quantum confinement.

$$\langle \Psi|p|0\rangle = N_\Phi \sum_{G_n} a(G_n) \int d^3r\, e^{i(G_n-k_0)r} f_e^*(r) f_h(r;S_{3/2}) + N_\Phi \sum_{G_n} b(G_n) \int d^3r\, e^{i(G_n-k_0)r} [\nabla f_e^*(r) + i(G_n-k_0) f_e^*(r)] f_h(r;S_{3/2}) , \tag{7}$$

with

$$a(G_n) = \frac{-i\hbar}{v_0} \int_{v_0} d^3r\, e^{-iG_n r} u^*_{ck_0}(r) \nabla u_{v0}(r) , \tag{8}$$

$$b(G_n) = \frac{-i\hbar}{v_0} \int_{v_0} d^3r\, e^{-iG_n r} u^*_{ck_0}(r) u_{v0}(r) , \tag{9}$$

where u_{ck_0} (u_{v0}) is the periodic part of the Bloch function ϕ_{ck_0} (ϕ_{v0}), G_n a reciprocal lattice vector, v_0 the volume of a unit cell, and the integrals in (8) and (9) are performed within a unit cell. In the first term of (7), the derivative of the periodic part of the Bloch function appears, whereas in the second term the derivative of the envelope function appears. Thus the contribution from the first term is generally larger than that from the second term. When the momentum matrix element is obtained, the radiative decay rate can be calculated using the well-known formula.[25]

The size dependence of the radiative lifetime of excitons is determined by the integrals in (7). In the case of Si and Ge, the conduction-band valleys are located near the zone boundary of the Brillouin zone and the magnitude of the wave vector $G_n - k_0$ is at least of the order of the inverse lattice constant. Thus the integrals take values of the order of unity only when the confinement size is as small as a few times the lattice constant and the envelope functions f_e and f_h have sizable Fourier components at the wave vectors of the same order of magnitude as $|G_n - k_0|$. As the quantum dot size is increased, the envelope functions become more and more flat and consequently the magnitude of the momentum matrix element and the radiative decay rate decrease rapidly.

In the calculation of (8) and (9), the Bloch functions in bulk crystals of Si and Ge are self-consistently determined by the first-principles local-density-functional method.[26,27] They are expressed by the linear combination of atomic orbitals form of the pseudoatomic wave function, which is obtained numerically in terms of a sum over Gaussian-type orbitals.[28,29,17] The calculated radiative decay rate of excitons in Si and Ge quantum dots is shown in Fig. 3 as a function of the quantum dot radius. The luminescence decay times of porous Si were reported to range from ns to ms.[5] If these time constants are considered as radiative recombination lifetimes, these values correspond to the quantum dot diameter ranging from 10 to 30 Å. These values are numerically different from those estimated from the luminescence peak energies.

However, there is a large size inhomogeneity about ±20 Å in diameter as can be estimated from the broad photoluminescence spectra.[3] Furthermore, the luminescence decay characteristics are determined by nonradiative processes as well as by the radiative decay. Especially, the nonradiative processes due to dangling bonds[30] at the nanostructure surface would contribute substantially to the luminescence decay. Thus the above discrepancy may be reconciled by taking into account ambiguities arising from these features. More systematic and intensive studies are necessary on the size dependence of the luminescence decay times before coming to a conclusion.

We can interpret the observed nonexponential behavior of the luminescence decay in terms of the size inhomogeneity of Si nanostructures and the presence of nonradiative relaxation channels. For example, in a quantum wire whose diameter is not uniform along the wire axis, an exciton localized at the thinner part having a relatively higher energy shows a faster luminescence decay but at the same time relaxes nonradiatively to the thicker part of the same quantum wire, where the exciton has a lower energy and shows a slower luminescence decay. These features can explain the nonexponential behavior of the luminescence decay.

In summary, we have investigated the quantum confinement effect on excitons in quantum dots of indirect-gap materials and clarified a mechanism which induces an indirect-to-direct conversion of the character of optical transition. The favorable agreement between the theory and experimental data on porous Si, concerning the blueshift of the exciton transition energy and the exciton binding energy, suggests strongly the importance of the quantum confinement effect in the luminescence processes of porous Si.

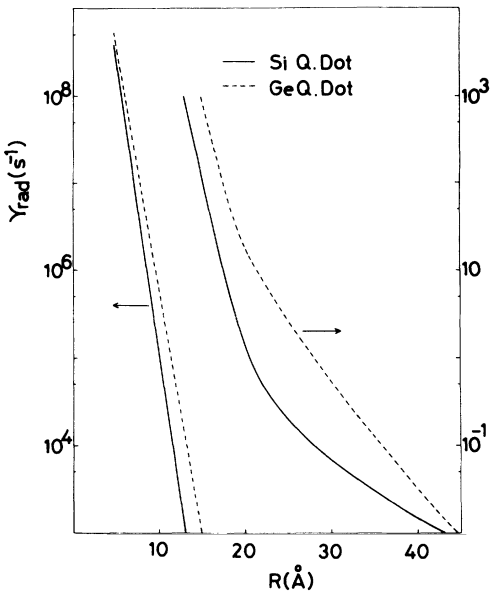

FIG. 3. The radiative decay rate of excitons in quantum dots is plotted as a function of the dot radius for Si (solid line) and Ge (dashed line).

The authors would like to thank Dr. L. T. Canham for providing us with detailed information on porous Si. They would also like to thank Dr. H. Kanbe, Dr. N. Uesugi, Dr. N. Matsumoto, and Dr. K. Shiraishi for helpful discussions and Dr. Y. Horikoshi, Dr. H. Hiratsuka, and Dr. T. Kimura for their encouragement.

[1]S. Furukawa and T. Miyasato, Phys. Rev. B **38**, 5726 (1988).
[2]H. Takagi, H. Ogawa, Y. Yamazaki, A. Ishizaki, and T. Nakagiri, Appl. Phys. Lett. **56**, 2379 (1990).
[3]L. T. Canham, Appl. Phys. Lett. **57**, 1046 (1990).
[4]V. Lehmann and U. Gösele, Appl. Phys. Lett. **58**, 856 (1991).
[5]*Light Emission from Silicon,* edited by S. S. Iyer, R. T. Collins, and L. T. Canham, MRS Symposia Proceedings No. 256 (Materials Research Society, Pittsburgh, 1991).
[6]M. Yamamoto, R. Hayashi, K. Tsunetomo, K. Kohno, and Y. Osaka, Jpn. J. Appl. Phys. **30**, 136 (1991).
[7]H. Morisaki, F. W. Ping, H. Ono, and K. Yazawa, J. Appl. Phys. **70**, 1869 (1991).
[8]S. Hayashi, M. Fujii, and K. Yamamoto, Jpn. J. Appl. Phys. **28**, L1464 (1989).
[9]Y. Maeda, N. Tsukamoto, Y. Yazawa, Y. Kanemitsu, and Y. Masumoto, Appl. Phys. Lett. **59**, 3168 (1991).
[10]K. P. Johansson, G. McLendon, and A. P. Marchetti, Chem. Phys. Lett. **179**, 321 (1991).
[11]H. Kanzaki and Y. Tadakuma, Solid State Commun. **80**, 33 (1991).
[12]U. Gnutzmann and K. Clausecker, Appl. Phys. **3**, 9 (1974).
[13]M. Kumagai, T. Takagahara, and E. Hanamura, Phys. Rev. B **37**, 898 (1988).
[14]T. P. Pearsall, J. Bevk, L. C. Feldman, J. M. Bonar, J. P. Mannaerts, and A. Ourmazd, Phys. Rev. Lett. **58**, 729 (1987).
[15]K. Takeda, K. Shiraishi, and N. Matsumoto, J. Am. Chem. Soc. **112**, 5043 (1990).
[16]P. J. Dean, J. Lumin. **1&2**, 398 (1970).
[17]K. Takeda and K. Shiraishi, Phys. Rev. B **39**, 11 028 (1989).
[18]J. M. Luttinger and W. Kohn, Phys. Rev. **97**, 869 (1955).
[19]J. M. Luttinger, Phys. Rev. **102**, 1030 (1956).
[20]W. Kohn, in *Solid State Physics,* edited by F. Seitz and D. Turnbull (Academic, New York, 1957), Vol. 5, p. 257.
[21]A. Baldereschi and N. O. Lipari, Phys. Rev. B **8**, 2697 (1973).
[22]T. Takagahara, Phys. Rev. B **36**, 9293 (1987).
[23]S. Gardelis, J. S. Rimmer, P. Dawson, B. Hamilton, R. A. Kubiak, T. E. Whall, and E. H. C. Parker, Appl. Phys. Lett. **59**, 2118 (1991).
[24]The relevant carrier masses are tabulated in, e.g., *Physics of Group IV Elements and III-V Compounds,* edited by O. Madelung, M. Schulz, and H. Weiss, Landolt-Börnstein, New Series, Group III, Vol. 17, Pt. a (Springer, Berlin, 1982).
[25]C. H. Henry and K. Nassau, Phys. Rev. B **1**, 1628 (1970).
[26]P. Hohenberg and W. Kohn, Phys. Rev. **136**, B864 (1964).
[27]W. Kohn and L. J. Sham, Phys. Rev. **140**, A1133 (1965).
[28]A. Oshiyama and M. Saito, J. Phys. Soc. Jpn. **56**, 2104 (1987).
[29]K. Shiraishi, A. Oshiyama, N. Shima, T. Nakayama, and H. Kamimura, Solid State Commun. **66**, 629 (1988).
[30]K. Takeda, K. Shiraishi, M. Fujiki, M. Kondo, and K. Morigaki (unpublished).